Investigation of Bio-Inspired Multi-Stage Architecture Effects on Lunar Mission Performance

Kristen Zack[1], and Tyler White[2]
School of ECAM, University of Georgia, Athens, Georgia, 30606, United States

Sydney Orlofsky[3]
School of ECAM, University of Georgia, Athens, Georgia, 30606, United States

William Talley[4]
School of ECAM, University of Georgia, Athens, Georgia, 30606, United States

Ramana Pidaparti[5]
College of Engineering, University of Georgia, Athens, Georgia, 30606, United States

Wayne Johnson[6]
School of ECAM, University of Georgia, Athens, Georgia, 30606, United States

Cargo delivery missions to the moon have an increasing need for architectures that manage landing robustness, launch performance, and efficient cislunar transport while assuring reliability. This student paper evaluates a multi-staged, bio-inspired cargo mission architecture where (i) a hybrid rocket chemically launches into low Earth orbit, (ii) cargo is transferred from LEO using an in-space propulsion system, and (iii) a landing interface inspired by the gripping style of a gecko optimizes surface attachment to the Moon when landing. To best quantify architectural benefit, key targets will include a 15% increase in hybrid fuel regression rate when compared to a straight port geometry, a 10-20% reduction in the propellant necessary to transport cargo relative to a baseline of an all-chemical transfer, and lastly a >20% performance improvement in a safety margin for landing relative to a baseline of friction-only pads for touchdown. Analytical models will establish preliminary results for capable parameters for this architecture; high-fidelity CFD is prioritized as the next step to further validate each stage's performance for an improved mission performance.

[1] Undergraduate Student, UGA ME, and AIAA University Student Member 1924200
[2] Undergraduate Student, UGA ME, and AIAA University Student Member 1922025
[3] Undergraduate Student, UGA ME, and AIAA University Student Member 1924751
[4] Undergraduate Student, UGA ME, and AIAA University Student Member 1931564
[5] Associate Fellow, Faculty Sponsor and Advisor
[6] Faculty Advisor

I. Introduction

In this study, a conceptual three-stage mission to the Moon is proposed where each stage employs a unique biologically inspired propulsion strategy customized to its tasked demands. The Moon offers well-defined mission stages, and clear performance baselines to generate operational comparisons. And, through evaluating these characteristics, quantitative evaluation and iterative optimization can exist against established staging models.

The chosen mission architecture is inspired by Artemis-era staging standards as well as modern cislunar operations concepts. This makes sure that there exists relevance to near-term exploration objectives. Our central objective is to identify and validate the gains in efficiency across all three mission stages. To achieve this, systematic biologically inspired improvements are intentionally integrated into pre-existing methodologies, appropriate to each stage's operational constraints and performance goals.

Biological systems have demonstrated their effectiveness through evolution, operating efficiently even when constrained by external factors such as mass, and environment. By emulating these naturally optimized strategies, the proposed methodologies draw on proven practical principles rather than relying solely on conventional, human-engineered solutions.

The applicability of this work extends beyond the hypothetical mission itself. It also allows for a structured way to include biologically inspired design into future space mission designs, creating opportunities to elevate efficiency and overall robustness. After proper evaluation, biologically inspired hypothetical missions can inform future propulsion system development and optimization efforts for operations to the Moon, as well as for more distant exploration architectures.

Despite these advantages, a multi-domain mission's performance is always constrained by limitations specific to each mission stage. For example, hybrid rocket engines suffer from inconsistent fuel regression rates and limited thrust scalability; cislunar transportation's dependence on high specific impulse is evident through long transit times; and landing on the Moon is a process sensitive to surface properties that create unstable margins for friction-dependent contact. These stage-specific constraints motivate the investigation of biologically inspired systems as a means to increase flexibility within otherwise rigid physical design requirements.

In addition to a high-Isp cislunar transfer strategy (Stage II), this paper assesses multiple bio-inspired design implementations, (i) a helical-port fuel grain geometry for launching off Earth (Stage I) and (ii) a gecko-inspired adhesion for landing on the Moon (Stage III), and further investigates how these stage-specific gains can improve a lunar cargo transport architecture. Using clearly defined objectives, we develop a first-order comparative framework and conduct preliminary cold-flow CFD analyses as a concept validation for Stage I. Quantitative performance targets are identified, and initial validation results are used to refine and guide further analysis.

II. Mission Architecture and Performance Metrics

A lunar cargo mission highlights an important systems-engineering problem: propulsion optimality is inherently phase-dependent. Every mission phase is controlled by different constraints. The launch phase needs high thrust, reliability, and impulse delivery to meet both ascent and mass-to-orbit requirements, whereas the cislunar transfer phase requires sufficient throttle and power availability, and propellant efficiency to support long-duration operations. In contrast, the final landing phase isn't driven as much by propulsion performance but instead by surface interaction, stability, and controllability under uncertain lunar terrain conditions.

The mission is thus intentionally subcategorized into three stages, for each to be investigated against appropriate physics-based criteria and performance metrics. By decomposing the mission, the system avoids becoming over constrained while maintaining a single, globally optimized propulsion solution. Figure 1 illustrates this architecture with three stages, which is assessed using phase-specific metrics that collectively roll up to overall mission performance and system-level effectiveness.

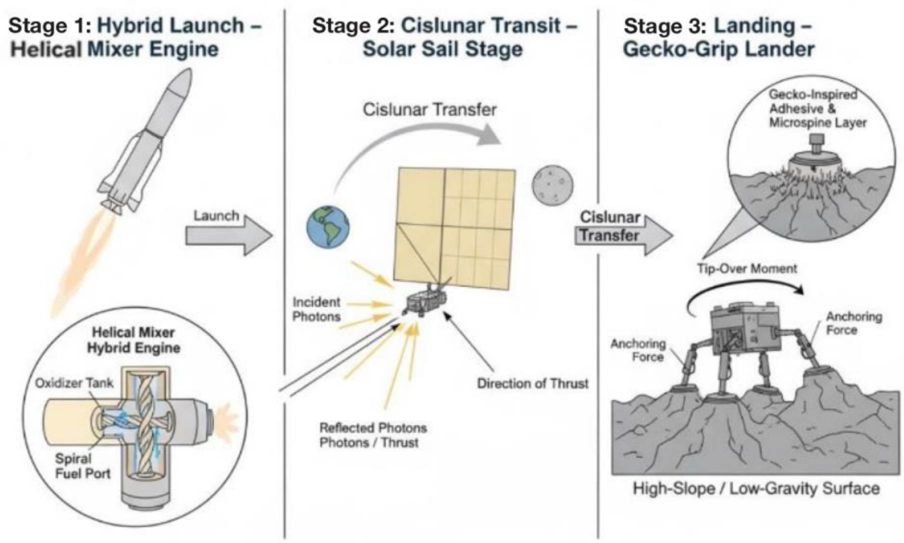

Figure 1. Bio-Inspired Three-Stage Lunar Cargo Architecture

A. Stage I – Earth Launch to Low Earth Orbit (Hybrid Rocket)

Historically a liquid-solid duopoly, propulsion offers varying attractive performance metrics to consider for launch. Liquid engines allow the engine to be throttled or even fully shut down, and they also have the best efficiency with the highest Isp of all engines at the cost of a more expensive and complex engine. On the other hand, solid engines are much easier to implement mechanically but lack throttle-ability and thus cannot be shut down once the engine is ignited, creating massive abort mode limitations and limiting the mission's flexibility. Like solids, hybrid rockets allow for safe storage since until oxidizer flow initiates, fuel is inert. They also allow for throttling to occur with oxidizer flow control, without the haphazard plumbing difficulties that a full liquid rocket architecture requires operation. Hybrid rockets, however, are still unfavorable in the aerospace community as they face a detrimental drawback: regression-rate-limited thrust scalability. For a fixed motor volume, a hybrid motor’s boundary-layer heat transfer and respective surface area of the fuel limits how quickly fuel can both mix and gasify – ultimately capping the maximum amount of achievable thrust a hybrid rocket can acquire upon launch.

Thus, this limitation transcends from the academic classroom into real aerospace architectures and acts as the primary reason hybrid engines are the least common launch system from Earth to space, despite exhibiting attractive operational capabilities that seem to combine the best characteristics of liquid and solid rocket engines. However, hybrid research conducted over the last two decades promises the revelation that hybrid regression limitations don’t have to be absolute – but rather that there is room for improvement. Many facets of research have thus been created. Liquefying (paraffin-based) fuels can allow for an unstable melting layer that incorporates droplets with the flow of the oxidizer and reports several times higher regression rates compared to baseline polymer fuels in scaled testing experiments [3]. In parallel, strategies for port shaping that optimize mixing and allow for secondary flow have shown great promise in leveraging the amount of effective heat transfer at the fuel surface for hybrid combustion. More specifically, helical port geometries – configuration made accessible increasingly by additive manufacturing – have improved overall mixing and targets high regression explicitly by combining helical features with hybrid fuel grains [4].

For a hybrid rocket port, a helical fuel grain introduces a three-dimensional shear and swirling motion near the hybrid port boundary (wall). By doing so, convective heat transfer is greatly increased compared to the baseline of a straight port. Instead of relying on mere geometry novelty, this evaluation focuses on whether the helical design will generate a shift in the regression correlation,

$$\dot{r} = aG^n \ ,$$

with a relative straight-port geometry oxidizer mass flux G. Through further analysis, the hybrid's helical port is evaluated by its repeatable and predictable regression performance (changes in a or n). From there, resulting implications can be presumed for both the total impulse and total thrust under fixed mass and sizing limitations.

B. Stage II – LEO to Cislunar Orbit (In-Space Propulsion)

The mission switches from a thrust-limitation issue to a mass-fraction problem once in orbit. While chemical propulsion can generate large ΔV in a short amount of time, it exhibits a low Isp that makes it more difficult to sustain the amount of propellant needed for longer journeys. Higher Isp options have the potential to reduce the propellant mass needed for cargo dramatically, but time-of-flight exists as a significant penalty for system implementation. This tradeoff becomes relevant to Artemis-era architectures and operations since NASA uses a lunar-proximal orbit (NRHO) staging approach that generates less operational stiffness for uncrewed missions [5]. To put in simpler terms: Stage II is where prioritizing a "slower but cheaper in propellant" mindset can become advantageous if the payload is uncrewed – which is appropriate for our chosen mission architecture.

C. Stage III – Lunar Landing (Gecko-Inspired Interface)

Landing is often evaluated in terms of optimizing propulsion and guidance, but when interested in transporting cargo, it is just as important to frame it as a surface interaction challenge. The Moon is home to a plethora of slopes; rough terrain, and uncertain regolith properties can hinder the working assumptions for a friction-only landing pad. By focusing on implementing bio-inspired dry adhesion, a new opportunity to control shear capacity becomes possible.

More importantly, this implementation is not simply speculative – gecko-inspired adhesive grippers were introduced onto NASA's Astrobee free-flying robot on the ISS to practice landing on a smooth surface under microgravity conditions [6], demonstrating one of the first on-demand detachment and attachment capabilities of gecko-inspired adhesion in a space environment [7]. In this paper, that concept is adapted to the Moon's landing surface – where success is not measured by stick duration but instead desiring an increased stability margin against potential rough terrain relative to commonly implemented friction-only pads [8].

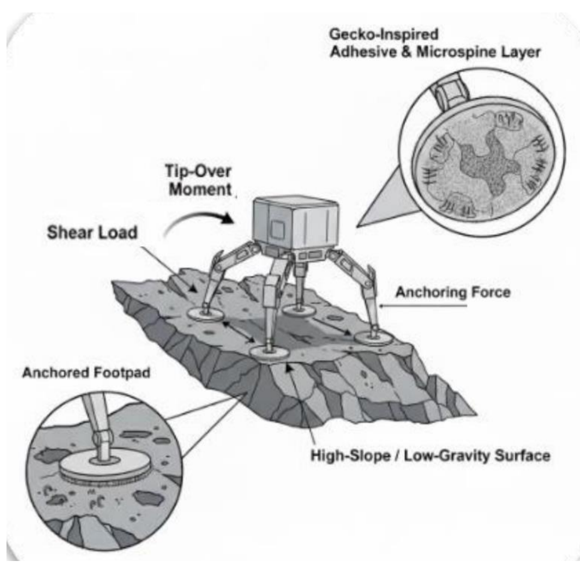

Figure 2. Conceptual Illustration of Gecko-Grip Lander

III. Bio-Inspired Design Approach

D. Hybrid Regression

In Section II, hybrid regression was explained to have a direct correlation to oxidizer mass flux and be dominated by the behavior evident at the boundary-layer. For instance, it becomes a more particular method of showing how transport near boundaries is in control of the amount of fuel mass added. Returning to a more classical hybrid theory approach, the oxidizer enters the chamber as the main flow and reacts in a diffusion flame located near the boundaries. Because of this, regression is mainly generated by convective heat transfer and is kept in balance by the respective energy needed to both vaporize fuel and upkeep a blowing motion into the flow of the port. And thus, this viewport is used later in this paper to support two different modeling choices: (i) comparisons for regression should be experimented at constant and equal oxidizer mass flux amounts, and (ii) shifts in regression parameters can be used to represent enhancements in geometric alterations.

Praised for its portable characteristics, the regression law is particularly valuable for mission analysis at a student-team level. Systematically, oxidizer flow is allowed to be swept over without having need of high-fidelity CFD for every point in the design. However, there exists a tradeoff: (a, n) must be justifiably proven with data from validated literature for the proposed fuel and oxidizer geometry. When further CFD analysis has been accumulated, it should be used as both as a mathematical validation and visual proof-of-concept, to show that the helical geometry for the port actually increases heat flux, and must agree with the calculated regression uplift assumed.

E. Helical Ports and Regression Approaches

The concept of a helical fuel grain port serves to address the hybrid-regression challenge of limited mixing. Geometries that enhance secondary motion would visibly and empirically optimize the heat transfer to the surface of the fuel. Instead of qualitative flow descriptions, "mixing enhancement" in literature is often preferred to be systematically measured. By far the most popular performance metric, regression uplift can be treated as a percent increase in regression rate expressed in the correlation between matched oxidizer mass flux.

Pursuant to our goal of using biology as a key inspiration, the helical grain is implemented as a bio-inspired mixing method in a higher level, functional way. Helical rotation is often witnessed in naturally occurring biological systems to create secondary swirling flow. This optimizes and strengthens mixing near wall boundaries in the combustion chamber. Bacterial flagellar propulsion is a widely accepted example, where twisting of the helical filament creates net axial motion that allows for fluid to continuously stay in motion (Fig. 3). The flagellum creates a net axial flow and secondary swirling rotation and is used in this paper as a functional demonstration for helical hybrid ports that generate secondary rotation to allow for better convective heat transfer and fluid mixing. The helical fuel design for launch therefore is inspired by the functional mechanism discussed, since it can introduce additional secondary mixing in the combustion chamber that reduces any stagnant regions, and maintains a steady mixing flow near boundaries.

In this paper, the performance of a helical port is evaluated as a controlled perturbation from a baseline port geometry (straight) under constant and equally comparable operating limitations. The bio-inspired helical feature is implemented to optimize convective transport compared to a baseline, straight port. The purpose of this paper is not to claim that a maximally optimized hybrid motor is ready for flight, as this study does not identify itself as a perfect architecture mission, but instead can be viewed as a viability study. Lastly, it is important to distinguish between two regression-optimization methods that are often analyzed: material-driven methods (like liquefying fuels previously mentioned), and geometry/flow-driven methods (swirl injection and helical ports). The present paper looks at the latter, while simultaneously recognizing that material selection may provide a legitimate alternative route to increasing regression behavior.

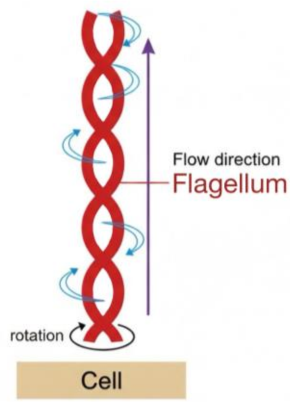

Fig. 3 Conceptual Illustration of Helical Flagellum

F. Cislunar Transport Architecture Context

The tension in designing an optimized cislunar cargo delivery lies in the tradeoff to achieve propellant savings. For instance, a chemical transfer stage would be able to implement very impulsive maneuvers and would deliver the cargo very quickly, which would reduce the time for potential exposure to risks in space. However, chemical transfers often have much lower Isp, which requires a need for much more propellant onboard. [9] Solar electric propulsion, by contrast, can greatly reduce the required propellant to transport a cargo payload. Biological inspired methods can also apply to its deployment, seeking inspiration from sailfish fins and other such methods. However, the flight duration would increase significantly and thus allow time for more system-level difficulties to procure. This results in a competition between operational simplicity and time (chemical propulsion), and optimal delivered mass (high Isp). What the "right" answer ends up depending on whether the payload is logistics-focused or time-critical.

Since, for this papers mission architecture, the primary metric is the in-space propellant needed to transport cargo from LEO to an orbit in close proximity to the Moon, solar electric propulsion (SEP) transfers are especially attractive. Stage II is viewed as a cargo logistics problem, instead of treating it as a crew transportation challenge. Under this payload assumption, there is much more flexibility in the allowable time-of-flight – as great as a few weeks to several months – given that the chosen and overall architecture reduces propellant mass onboard and increases the amount of payload delivered [9]. SEP allows for high Isp and demands much less propellant, important for missions like this one where logistics cadence is more important than arriving quickly.

G. Gecko-Inspired Adhesion for Space Contact and Perching

Alongside serving as a biological curiosity, gecko-inspired dry adhesives demonstrate a more controlled surface-interaction mechanism that is increasingly relevant as spacecraft contact tasks become imperative for space exploration. Foundational biomechanics paved the way for establishing how gecko attachments are unusual from an engineering perspective. Often described as "frictional adhesion", adhesion is an extremely directional property and is often coupled to shear loading [10]. This allows for low detachment forces when appropriately unloaded and equally strong attachment in the shear direction preferred [11]. This "stickiness" is highly sought out in robotic interactions, as it creates a more controllable interaction rather than a permanent attachment. In the Stanford climbing-adhesion paper, these biological principles were translated into synthetic directional adhesives and showed force-control strategies and dictional engagement requirements for robust attachment and detachment cycles on smooth surfaces [12]. Fig. 2 provides an illustrative, conceptual design of a gecko-gripper lander, where the biological principles mentioned above directly translate to increased anchoring force upon low-gravity surfaces.

Critically, gecko-inspired adhesives are very relevant to modern space systems. Gecko-inspired grippers were put on NASA's Astrobee robot on the ISS, setting the precedent for such a modern controlled attachment [7]. Translating this landing capability is foundationally mechanical: by treating adhesion as controllable to resisting shear stress at the Moon's surface (contact interface). This thereby increases the margin against falling/slipping when the landing regolith and respective friction is unknown. To put it simply, when relying on friction as the point of contact, the resisting capacity μN is provided. However, adhesion-enabled interfaces (like gecko-inspired dry adhesives) can be represented as $\mu N + F_{adh}$, where F_{adh} models the amount of controllable shear adhesion available [7].

IV. Methods for Modeling and Analysis

This section analyses workflows used across the three stages to evaluate architecture effects. Stage I is modeled in the most detail comparatively since it acts as the main technical lever in the overall mission architecture. The mission is designed around the Space Launch System, whose performance specifications can be defined by its thrust of 8.8 million lbs. [1] and its Isp of 452 s [2]. Thus, Stages II and III use lightweight first-order equations for comparison against standardized baselines.

H. Stage I: Hybrid Regression Framework

Hybrid regression is represented using the boundary-layer driven perspective: oxidizer enters as the primary core flow, and combustion dominates a near-boundary diffusion. [13] From there, regression is determined by convective transfer to the surface of the fuel with the energy needed to both vaporize the fuel into the port opening. [13] This representation paints the picture of the canonical turbulent boundary-layer hybrid theory, showing that regression in the combustion chamber is largely correlated to oxidizer mass flux instead of the chamber's respective pressure. [14] This was observed primarily using the mass-flux correlation from earlier,

$$\dot{r} = aG^n ,$$

with the calculated oxidizer mass flux as follows,

$$G = \frac{\dot{m_{ox}}}{A_{port}} ,$$

Where A_{port} is the cross-sectional area of the combustion chamber port. [15] The amount of added fuel mass can be interpreted as

$$\dot{m_f} = \rho_f A_{burn} \dot{r} ,$$

Where A_{burn} is the surface area that burns due to the geometry of the port (whether it is straight or helical will greatly alter this resultant value). The relationships above allow for parametric sweeps without needing different CFD runs at varying design-point stages.

Therefore, in this paper CFD is used as a mechanism check rather than the core predictor of regression, maintaining a theoretical and numerical validation of helical implementation. Fig. 4 shows the Inventor design used as a baseline for the main geometric parameters – such as the diameter and length of the port - establishing a strong body for further computation in Stage I.

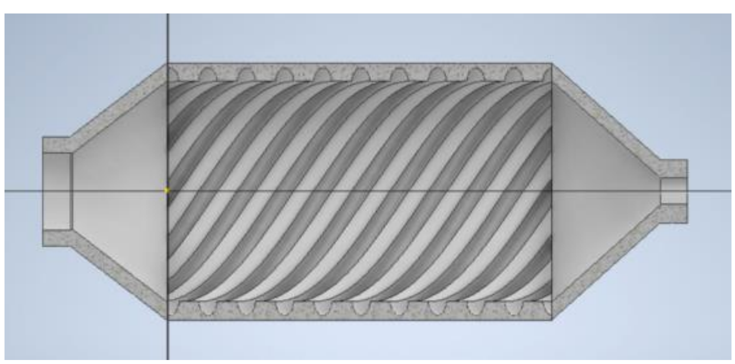

Fig. 4 Preliminary Hybrid Engine Barrel Model

I. Stage II: First-Order Cislunar Propellant Comparison

Stage II's requirements are treated at a mission-relevance level: the propellant necessary to move cargo from LEO to a lunar-proximal orbit. Since Artemis-era architectures typically use NRHO as the lunar staging orbit, for operational flexibility NRHO is also used as this mission's "delivery orbit" [16]. This choice keeps comparative mass budgeting constant, instead of pushing for a vague "efficiency" requirement. The impulsive rocket equation serves as the baseline for chemical transfer,

$$\frac{m_0}{m_f} = \exp\left(\frac{\Delta V}{g_0 I_{sp}}\right) \quad ,$$

Creating a demand under a predetermined ΔV and Isp. For an uncrewed payload, the duration of flight is not a primary constraint, and thus a transfer duration of 30-120 days is proposed to allow for cargo-appropriate delivery rather than time-critical crew transportation. [17] For this reason, SEP-class transfers are attractive for their reduced propellant demand potential in an all-chemical propulsion mission.

SEP and similar electric propulsion technology are relatively recent developments in the aerospace industry, and as such there is a substantial lack of literature regarding SEP systems or methodology by which to analyze and improve electric propulsion parameters beside thrust output. Projects like NASA's SEP project at Glenn Research Center may serve as reference points for future SEP analysis [9].

J. Stage III: Landing Interface Stability Margin

Using a simplified slip-resistance model, Stage III's landing robustness is evaluated to answer the following architecture question: When friction is uncertain, how much stability can adhesion provide? By creating a ratio between the friction-only baseline,

$$F_{resist} = \mu N \quad ,$$

and the adhesion-enabled interface,

$$F_{resist} = \mu N + F_{adh},$$

performance can thus be measured as a marginal improvement with respect to friction-only contact. This can be defined as the ratio:

$$M = \frac{F_{resist,\text{adh}}}{F_{resist,\text{fric}}} = 1 + \frac{F_{adh}}{\mu N}$$

V. Results and Discussion

Preliminary CFD results calculated to support Stage I's "mechanism check" were evaluated to answer the following question: would implementing a helical port produce flow features that align with an increase in near-wall transport versus a straight port under consistent inlet conditions? To this effect, cold-flow, steady simulations were generated and are not supposed to directly predict combustion performance. However, they do serve as evidence for the predicted changes in the regression framework through a comparison of velocity structure, pressure-drop, and wall shear stress between the two competing geometries.

Our preliminary baseline case consisted of a straight cylindrical port. The resultant solution converged with a steady and balanced inlet/outlet mass flow rate ($\dot{m}_{in}$ = 9.559x10^{-4} kg/s and $\dot{m}_{out}$ = -9.559x10^{-4} kg/s). The straight-port baseline had an area-weighted inlet static pressure of 40.0 Pa higher than the outlet, and its flow field had a largely axial core with a maximum velocity of approximately 12.7 m/s (as shown in the straight-port velocity contour figure). The area-weighted average wall shear stress for the straight port is τ_w = 0.629 Pa, with a peak wall shear of 0.844 Pa on the wall boundary.

Under the same general inlet and outlet conditions, the helical port case was then simulated. In comparison to the straight port, the helical port had a considerably higher pressure drop: the area-weighted pressures were reported as P_{in} = 433.4 Pa and P_{out} = 57.2 Pa – close to a 9.4x increase in comparison to the straight-port geometry baseline. However, the helical port flow simulated a much stronger three-dimensional streamline/pathline output, as secondary motion was visually noted with the maximum velocity reaching around 15.3 m/s (~20% of an increase compared to the straight-port maximum). Also, and more importantly when discussing regression optimization, the near-wall momentum-transfer proxy was increased by using the helical port: the area-weighted average wall shear stress increased from τ_w = 0.629 Pa (for the straight port) to τ_w= 0.7365 Pa (for the helical port). This ~17% increase in τ_w is consistent with the manuscript's modeling assumption that geometric alterations can "uplift" effective regression behavior and induce secondary motion when compared against a straight-port, since hybrid regression is dominated by the behavior of the boundary-layer and near-wall transport. Table 1 summarizes the CFD outputs discussed in this preliminary analysis.

Table 1. Preliminary CFD Metrics (Cold-Flow "Mechanism Check")

Geometry	$\dot{m}$ (kg/s)	Δp (Pa)	$\bar{\tau}_w$ (Pa)	V_{max} (m/s)
Straight Port (Baseline)	9.56×10^{-4}	40	0.629	12.7
Helical Port (Featured)	9.56×10^{-4} *(matched intent)*	376	0.7365	15.3

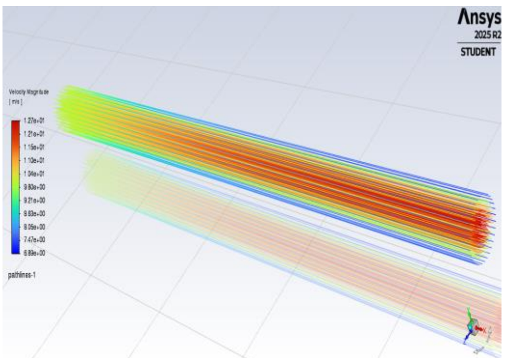

Figure 5. Straight-Port Velocity Contour

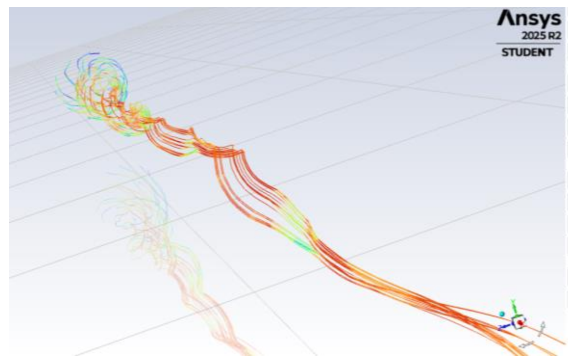

Figure 6. Helical-Port Velocity Streamlines

These CFD simulations should be interpreted as a mechanism check, not advanced regression-rate prediction models as the simulations were modeled for cold-flow testing. Regardless, helical geometry produced two valuable outcomes: (i) an increase in near-wall transport proxy, with a discerning wall shear rising, and (ii) pressure drops under matched mass-flow intent. The resultant increase in secondary-flow directly aligns with the previously represented regression framework and shows the helical-port effects (like uplift) visible in Fig. 6 as a geometry-driven benefit. The helical port – for the proposed mission architecture - is defined as a Stage I trade, as at the expense of greater pressure loss, near-wall transport was improved. This can sufficiently be carried into more expansive validation of design and comparison.

VI. Limitations and Future Work

This paper is intentionally structured as an architecture-effects study supported by concepts and preliminary CFD analysis. As a result, the mission-level conclusions should be interpreted as conceptual rather than conclusive. The intent is to identify which architectural and design aspects are worth pursuing, and to estimate their relative influence, rather than immediate integrability of any proposed subsystem. In the absence of physical prototypes or experimental validation, the conclusions presented are necessarily theoretical and are best viewed as motivating opportunities for future testing and refinement.

Stage I represents both the primary technical limitation and the greatest opportunity within the proposed architecture. Literature-based hybrid rocket correlations are used to model regression-rate enhancement and geometry-driven perturbations. However, the specific helical port geometry shown in Fig. 4 has not yet undergone a comprehensive validation analysis to support its structural or operational deployment. The associated cold-flow CFD analysis is intended as a mechanism-level check to support enhanced near-boundary mixing, not as a predictive model. Consequently, without additional testing, the reported parameters remain sensitive to injector boundary conditions and manufacturing tolerances that may alter the intended port geometry. Stage I results should therefore be interpreted as design targets and performance bounds, rather than finalized regression laws for a specific manufacturing configuration. Stages II and III are likewise constrained by the deliberate use of first-order modeling approaches. While appropriate for an architectural-level investigation, these simplifications preclude detailed treatment of operational constraints, trajectory-optimized low-thrust transfers beyond indicative time-of-flight estimates or closed-loop guidance considerations. Similarly, the gecko-inspired landing interface is evaluated at a conceptual level and does not attempt to model full landing dynamics or potential degradation mechanisms such as regolith contamination. These limitations define clear pathways for future work, where higher-fidelity modeling and experimental validation can be applied to mature the concepts introduced here.

Future work should focus on validation efforts that prioritize the most influential impact at each mission stage, as is the paper's mission focus. In the future, Stage I development should include (i) a parametric CFD sweep over port diameter, oxidizer mass flux, helix pitch, and helix depth to quantify changes in wall heat flux, and (ii) translation of these effects into corresponding shifts in the effective regression parameters. This approach ties the paper's primary objective together, by demonstrating an empirical regression-rate increase relative to a straight-port baseline. Section V can then be extended to incorporate both nominal performance predictions and expanded uncertainty bounds, such as distributions of regression-rate uplift. These future works and the bio-inspired "mechanism levers" to evaluate quantitatively will have an impact on overall mission-level architecture performance.

VII. Conclusion

A multi-stage, bio-inspired lunar cargo architecture was investigated to optimize hybrid launch performance, cislunar travel, and landing under varying mission requirements and constraints. Mission-level metrics - especially a 15% regression-rate increase - was defined for future mission architectures to have a comparative success baseline. In this paper, preliminary cold-flow CFD comparisons for Stage I exist to be expanded upon, whist serving as baseline proof that helical geometric features can improve near-wall transport proxies, at the cost of an increase in pressure drop. Future work will prioritize completing helical-port CFD refinement and regression uplift, while evaluating Stage II and III further with higher-fidelity models.

References

[1] Sauers, Elisha. "Is SLS Still the Most Powerful Rocket? 5 Facts as Artemis 2 Rolls Out." *Mashable*, Mashable, 17 Jan. 2026, mashable.com/article/nasa-sls-artemis-2-rollout-facts. https://mashable.com/article/nasa-sls-artemis-2-rollout-facts

[2] L3Harris Technologies, "RS-25 Engine," L3Harris, https://www.l3harris.com/all-capabilities/rs-25-engine

[3] Karabeyoglu, A., Zilliac, G., Cantwell, B. J., DeZilwa, S., and Castellucci, P., "Scale-Up Tests of High Regression Rate Paraffin-Based Hybrid Rocket Fuels," Journal of Propulsion and Power, Vol. 20, No. 6, 2004, pp. 1037–1045. doi:10.2514/1.3340.

[4] Walker, S. M., Helical Port Geometry Fuel Grains for Hybrid Rockets, M.S. Thesis, Mechanical and Aerospace Engineering Dept., Utah State Univ., Logan, UT, 2015.

[5] Esty, C. C., et al., "Assessment of Cislunar Staging Orbits to Support the Artemis Campaign," AAS Paper 22-762, 2023. NASA Technical Reports Server (NTRS). URL: https://ntrs.nasa.gov/api/citations/20220011365/downloads/AAS%2022-762.pdf

[6] Chen, T. G., Cauligi, A., Suresh, S. A., Dille, M., Garcia Ruiz, R., Mora Vargas, A., Pavone, M., and Cutkosky, M., "Testing Gecko-Inspired Adhesives with Astrobee Aboard the International Space Station: Readying the Technology for

Space," IEEE Robotics & Automation Magazine, 2022. URL: https://ramagazine.ieee.org/2022/10/24/testing-gecko-inspired-adhesives-with-astrobee-aboard-the-international-space-station-readying-the-technology-for-space/

[7] National Aeronautics and Space Administration, "Astrobee Tests Gecko-Inspired Adhesives in Space," NASA, May 18, 2021. URL: https://www.nasa.gov/image-article/sticking-around-astrobee-tests-gecko-inspired-adhesives-space/

[8] Cauligi, A., Chen, T. G., Suresh, S. A., Dille, M., Garcia Ruiz, R., Mora Vargas, A., Pavone, M., and Cutkosky, M., "Design and Development of a Gecko-Adhesive Gripper for the Astrobee Free-Flying Robot," in Proceedings of the International Symposium on Artificial Intelligence, Robotics and Automation in Space (i-SAIRAS), 2020. URL: https://www.hou.usra.edu/meetings/isairas2020fullpapers/pdf/5055.pdf

[9] NASA. Solar Electric Propulsion - NASA. (2023, May 8). NASA. https://www.nasa.gov/space-technology-mission-directorate/tdm/solar-electric-propulsion/

[10] Sameoto, D., and Menon, C., "Recent Advances in the Fabrication and Adhesion Testing of Biomimetic Dry Adhesives," Smart Materials and Structures, Vol. 19, No. 10, 2010, Article 103001. doi:10.1088/0964-1726/19/10/103001.

[11] Sikdar, S., Rahman, M. H., Siddaiah, A., and Menezes, P. L., "Gecko-Inspired Adhesive Mechanisms and Adhesives for Robots—A Review," Robotics, Vol. 11, No. 6, 2022, Article 143. doi:10.3390/robotics11060143.

[12] Santos, D., Spenko, M., Parness, A., Kim, S., and Cutkosky, M., "Directional Adhesion for Climbing: Theoretical and Practical Considerations," Journal of Adhesion Science and Technology, Vol. 21, 2007, pp. 1317–1341. doi:10.1163/156856107782328399.

[13] Marxman, G. A., and Gilbert, M., "Turbulent Boundary Layer Combustion in the Hybrid Rocket," Symposium (International) on Combustion, Vol. 9, No. 1, 1963, pp. 371–383. doi:10.1016/S0082-0784(63)80046-6.

[14] Chiaverini, M. J., Serin, N., Johnson, D. K., Lu, Y.-C., Kuo, K. K., and Risha, G. A., "Regression Rate Behavior of Hybrid Rocket Solid Fuels," Journal of Propulsion and Power, Vol. 16, No. 1, 2000, pp. 125–132. doi:10.2514/2.5541.

[15] Zilliac, G., and Karabeyoglu, M. A., "Hybrid Rocket Fuel Regression Rate Data and Modeling," AIAA Paper 2006-4504, 2006. doi:10.2514/6.2006-4504.

[16] Lee, D. E., "Gateway Destination Orbit Model: A Continuous 15 Year NRHO Reference Trajectory," NASA, 2019.

[17] Manzella, D., et al., "High-Power Solar Electric Propulsion for Future NASA Missions," NASA, 2014.